Research Article Vol. 2, No. 11 / November 2015 / Optica 944

Generating ultrafast pulses of light from quantum cascade lasers

Feihu Wang,[1] Kenneth Maussang,[1] Souad Moumdji,[2] Raffaele Colombelli,[2] Joshua R. Freeman,[3] Iman Kundu,[3] Lianhe Li,[3] Edmund H. Linfield,[3] A. Giles Davies,[3] Juliette Mangeney,[1] Jérôme Tignon,[1] and Sukhdeep S. Dhillon[1,*]

[1]Laboratoire Pierre Aigrain, Ecole Normale Supérieure-PSL Research University, CNRS, Université Pierre et Marie Curie-Sorbonne Universités, Université Paris Diderot-Sorbonne Paris Cité, 24 rue Lhomond, 75231 Paris Cedex 05, France
[2]Institut d'Electronique Fondamentale, Univ. Paris Sud, CNRS UMR8622, 91405 Orsay, France
[3]School of Electronic and Electrical Engineering, University of Leeds, Woodhouse Lane, Leeds LS29JT, UK
*Corresponding author: sukhdeep.dhillon@lpa.ens.fr

Received 26 June 2015; revised 5 October 2015; accepted 7 October 2015 (Doc. ID 243824); published 4 November 2015

The generation of ultrashort pulses from quantum cascade lasers (QCLs) has proved to be challenging. It has been suggested that the ultrafast electron dynamics of these devices is the limiting factor for mode locking and, hence, pulse formation. Even so, the clear mode locking of terahertz (THz) QCLs has been demonstrated recently, but the exact mechanism for pulse generation is not fully understood. Here we demonstrate that the dominant factor necessary for active pulse generation is in fact the synchronization between the propagating electronic modulation and the generated THz pulse in the QCL. By using the phase-resolved detection of the electric field in QCLs embedded in metal–metal waveguides, we demonstrate that active mode locking requires the phase velocity of the microwave round-trip modulation to equal the group velocity of the THz pulse. This allows the THz pulse to propagate in phase with the microwave modulation along the gain medium, permitting short-pulse generation. Mode locking was performed on QCLs employing phonon depopulation active regions, permitting the coherent detection of large gain bandwidths (500 GHz) and the generation of 11 ps pulses centered around 2.6 THz when the above "phase-matching" condition is satisfied. This work brings an enhanced understanding of QCL mode locking and will permit new concepts to be explored to generate shorter and more intense pulses from mid-infrared, as well as THz, QCLs.

OCIS codes: (140.0140) Lasers and laser optics; (140.5960) Semiconductor lasers; (140.5965) Semiconductor lasers, quantum cascade; (140.4050) Mode-locked lasers.

http://dx.doi.org/10.1364/OPTICA.2.000944

1. INTRODUCTION

Terahertz (THz) frequency quantum cascade lasers (QCLs) [1] are semiconductor devices based on inter-sub-band transitions that can emit over the ~1–5 THz spectral range. There have been considerable developments in the performance of these sources in recent years, including significant increases in output power [2] and operating temperature [3]. Since the ultrafast gain recovery time inherent to QCLs is considerably shorter than the round-trip cavity time [4], it has been believed that these devices cannot be mode-locked (multiple pulses are generated within the QCL cavity) and, thus, unable to generate short pulses. However, it has been shown recently that these devices can be actively mode-locked, where the QCL is modulated at microwave frequencies, to generate a train of picosecond pulses [4–6]. Nonetheless, the exact mechanism that permits pulse generation is not fully understood, unlike interband lasers where active mode locking has been extensively investigated and is well known [7–9]. For example, it is not clear why THz QCLs are easier to mode-lock when compared with those operating in the mid-infrared. A further challenge to understanding QCL mode locking in the THz frequency range is that all demonstrations to date have been based on QCLs employing bound-to-continuum active region designs and fabricated in single-plasmon waveguides. These active regions were used as they have low electrical power requirements, thus permitting CW operation (or high duty cycles), whereas the single-plasmon waveguides help provide high output powers. However, this has restricted insight into the mode locking mechanism. For example, this active region leads to small spectral bandwidths (~100 GHz), and so the effect of the bandwidth on the pulse generation has not been investigated. Furthermore, no consideration has been made on the suitability of the single-plasmon THz waveguide for guiding the microwave modulation.

In this article, we demonstrate active mode locking through injection seeding of THz QCLs based on the longitudinal-optical

(LO) phonon depopulation active region scheme, embedded in metal–metal (MM) waveguides. These active regions provide large emission bandwidths, greater than 500 GHz, and the MM waveguide confines both the microwave modulation and THz emission. Using this large bandwidth, we demonstrate that the actively mode-locked pulse width is principally determined by the microwave frequency modulation, rather than being limited by the gain bandwidth, and show that the microwave phase velocity needs to be equal to the THz group velocity for pulse generation. The active mode locking method reported here, in contrast to the mode locking demonstrations in Ref. [5], also limits the pulse generation close to the lasing threshold owing to the direct modulation of the gain above and below the threshold through the entire cavity. The fast direct modulation is permitted by the ultrafast gain recovery time, which we determine experimentally to be ~5 ps, approaching that of mid-infrared QCLs (~1 ps).

2. SAMPLE

A QCL with an LO phonon depopulation scheme was used, based on a 3.1 THz QCL, which has been shown to operate up to 200 K [3]. The design was modified to operate at lower frequencies (~2.6 THz) by increasing the well and barrier widths, thereby improving the spectral overlap with the THz seed pulse [10]. Starting from the injection barrier, the well and barrier widths were *4.6*/9.8/*2.6*/9.0/*4.4*/17.6 nm (barriers in italic). The 17.6-nm-wide well was n-doped at a level of 5×10^{16} cm^{-3} over the central 5 nm.

The growth was performed using molecular beam epitaxy. The wafer was processed into 3-mm-long laser ridges in MM waveguides using standard photolithography. This type of waveguide, coupled with the LO phonon depopulation active region design, provides state-of-the-art THz QCL temperature performance. Ridge widths of 60 μm were selected to suppress higher lateral modes such that the fundamental mode dominates the laser action [11], important for active mode locking to avoid multiple pulses within the cavity. The QCL was coupled with a high-speed mount for gigahertz (GHz) frequency modulation [see the inset of Fig. 4(c)] and placed in a continuous-flow cryostat. At 77 K, the laser threshold is observed at 722 A/cm^2 and lasing ceases at 998 A/cm^2 with a duty cycle of 6%. Figure 1 shows the light–current–voltage (LIV) characteristics of the QCL, using a pyroelectric detector to measure the output power. Laser action is observed up to 130 K with a duty cycle of 6%. The electrical characteristics are typical for this type of active region. The inset of Fig. 1 shows the calculated mode profiles in facet and surface views confirming that only one lateral mode is present.

3. INJECTION SEEDING

Prior to mode locking, a technique based on ultrafast injection seeding was employed to measure the time-resolved electric field emitted by the QCL. THz frequency pulses, of bandwidth ~3 THz, were generated using a photoconductive antenna excited by 100 fs near-infrared pulses (centered at ~800 nm) from a Ti:sapphire laser. These free-space THz pulses were injected into the MM QCL cavities using high-numerical-aperture parabolic mirrors, enabling the injection seeding of the QCL and permitting the coherent detection of its emission. The THz pulse injection is synchronized with an electrical RF pulse that switches on the QCL, triggered by the same 100 fs near-infrared pulses.

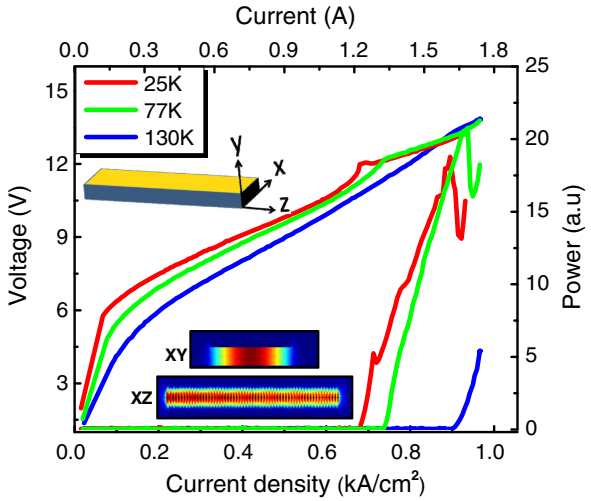

Fig. 1. Light–current density–voltage characteristics of the 2.6 THz MM waveguide QCL based on an LO phonon depopulation active region at 25 K (red), 77 K (green), and 130 K (blue). Top inset: schematic diagram showing the QCL coordinate system XYZ. Bottom inset: transverse (XY) and longitudinal (XZ) mode simulations of the THz mode profile inside the MM waveguide QCL.

This allows the THz input pulses to be amplified and eventually seed the QCL emission, rather than the emission being initiated by the QCL's inherent spontaneous emission. Electro-optic sampling was then used to measure the amplitude and phase of the QCL emission. Further details of the technique can be found in Ref. [10]. (The time-resolved output intensity of an unseeded QCL can be measured using the cross-polarizer technique [12], but is orders of magnitude less sensitive compared with that using the seeded technique. It is thus not suited to the low output power of MM QCLs.)

Figure 2(a) shows the measured electric field as a function of time for a QCL injected with an ultrafast THz seed pulse, at 77 K. The QCL was held below the threshold with a quasi-DC current of 609 A/cm^2 with a 3.6 ns electrical switching pulse used to bring the QCL above the threshold, the latter synchronized with the THz seed pulse. The seeding THz pulse is injected into the QCL through one of its facets at $t = 64$ ps and is amplified as it propagates along the laser cavity. At the output facet, part of the pulse is transmitted and detected coherently, whereas the remainder is reflected back into the cavity and continues to be amplified. The pulse is again reflected at the input facet. This results in successive pulses exiting the QCL output facet, which increase in field amplitude, separated by the cavity round-trip time of 76 ps corresponding to a refractive index of 3.665. Subsequently (>300 ps), complex behavior emerges with weaker emission observed between the round-trip pulses, as seen previously in bound-to-continuum devices [10,13]. This is a result of a number of longitudinal modes present in a long cavity [14] and the ultrafast gain recovery time (see below). Furthermore, owing to the finite gain bandwidth of the QCL, the input THz pulse is broadened in time with the number of round trips, resulting in the output pulses becoming less distinguishable at later times (>400 ps). A magnified view of the output emission around 430 ps is highlighted in Fig. 2(b), which clearly shows the time-resolved form of the electric field with a resolution of

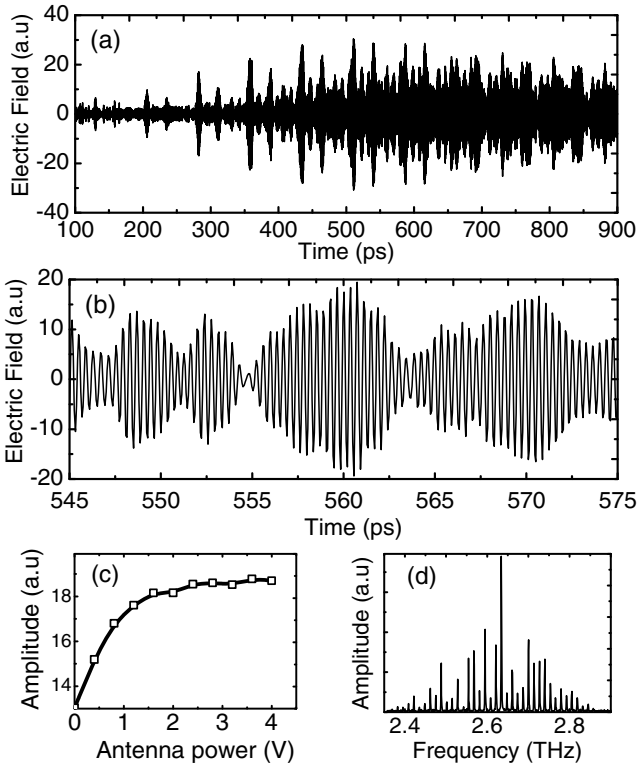

Fig. 2. Injection seeding of the MM waveguide QCL at 77 K. (a) Emitted electric field from the QCL as a function of time with a bias of 3 V on the seed antenna. (b) Expanded view of the emitted QCL electric field between 545 and 575 ps. (c) QCL output field amplitude at 431 ps as a function of the voltage applied on the THz photoconductive antenna. (d) FFT of the QCL output electric field.

30 fs. (The inter-round-trip pulses can be inhibited when using active mode locking as detailed below.)

After ∼400 ps, corresponding to six round trips, there is no further amplification of the output electric field. (The small reduction in amplitude after 700 ps is a result of the electrical switching pulse not being perfectly flat.) Although the stabilization of the field is an indication that the QCL is entirely synchronized with the input pulse, the variation of the output field was investigated as a function of the input THz field to confirm this. Figure 2(c) shows the QCL output field at a time of 431 ps as a function of voltage on the THz antenna, with similar behavior observed for later times. (The electric field emitted by the antenna is proportional to the applied voltage [10].) For applied fields greater than ∼2 V, the QCL output field saturates, implying that the QCL gain is clamped by the THz input pulses, with the latter therefore initiating (i.e., seeding) the laser action, replacing entirely the inherently random spontaneous emission of the QCL. (A small unsynchronized part of the electric field may still be present, but this will be considerably smaller than the synchronized field [13] and, in the case of mode locking, will have a similar time profile [12].). For antenna voltages <2 V, however, the measured QCL output field depends on the input THz pulse amplitude. This implies that only amplification of the input THz pulse is detected with contributions to the QCL output from the seed and spontaneous emission [13].

Figure 2(d) shows the fast Fourier transform (FFT) of the measured time-domain signal in Fig. 2(a), permitting access to the QCL output spectrum. The spectrum is centered at ∼2.6 THz with a bandwidth greater than 500 GHz, considerably larger than that in previous demonstrations (100 GHz), owing to the large spectral gain of LO phonon depopulation active region designs. The mode spacing is 13.2 GHz as expected for a 3-mm-long waveguide. Furthermore, the frequency of each Fabry–Perot mode is linear with mode number, demonstrating that the QCL is operating on only one lateral mode and there are no higher-order-modes present. The microwave beat note was also measured, which showed a narrow linewidth at only one frequency at the round trip just above the laser threshold, which gradually became wider with increasing current. Similar behavior of the beat note has been demonstrated previously in, for example, Ref. [15].

By comparing the measured time profile in Fig. 2(a) to Maxwell–Bloch time-domain simulations, an estimate of the gain recovery time of the QCL can be obtained. Using the procedure presented in Ref. [14] with a dephasing time of 0.6 ps and a total waveguide loss of 12 cm^{-1}, a gain recovery time of ∼5 ps is determined. Further details of the parameters used can be found in Supplement 1. This is considerably faster than for bound-to-continuum devices, which have gain recovery times of ∼15 ps, and is considerably shorter than the round-trip time (76 ps). (Note that the gain recovery time for mid-infrared QCLs is of the order of ∼1 ps [16,17].). The shorter gain recovery time is also indicated in the time-resolved electric field [Fig. 2(b)], which shows multiple "pulses" between cavity round trips separated between 5 and 7 ps. This is a result of the faster dynamics of the LO phonon depopulation designs and owing to the absence of a miniband for interperiod transport.

4. ACTIVE MODE LOCKING

Using this injection seeding technique, the mode locking of QCLs was investigated with the expectation that the large bandwidth available in these devices should lead to shorter pulses in comparison with mode-locked bound-to-continuum active region designs [6]. Specifically, pulses as short as 1 ps would be expected from a seeding bandwidth of 500 GHz, assuming transform-limited pulses. To actively mode-lock the QCL, a microwave modulation was applied corresponding to the round-trip time (i.e., ∼13 GHz for a 3-mm-long cavity) to modulate the gain across the entire gain medium. (Note that it is also possible to modulate a short section of the cavity at the round-trip frequency to actively mode-lock a QCL to open a picosecond time window in the net gain, as in Ref. [4]. However, this requires a specially designed QCL with a long gain recovery time.) The bonding wire on top of the QCL is placed close to the facet onto which the external THz pulse is incident [see the inset of Fig. 4(c)]. In this case, the microwave modulation will propagate between the input and output facets together with the seed pulse, allowing the QCL to be seeded and mode-locked for pulse generation. No pulse generation is observed when the bonding wire is placed in the middle of the QCL cavity as this results in a counter-propagating modulation.

The experimental arrangement for active mode locking is the same as that reported in Ref. [6], where a yttrium iron garnet bandpass filter is employed to choose a harmonic of the reference laser repetition rate (for example, the 163 harmonic × 76.47 MHz = 12.46 GHz) to synchronize the round-trip microwave modulation of the QCL with the seeding pulses. A microwave power of 30 dBm was used. This is the maximum

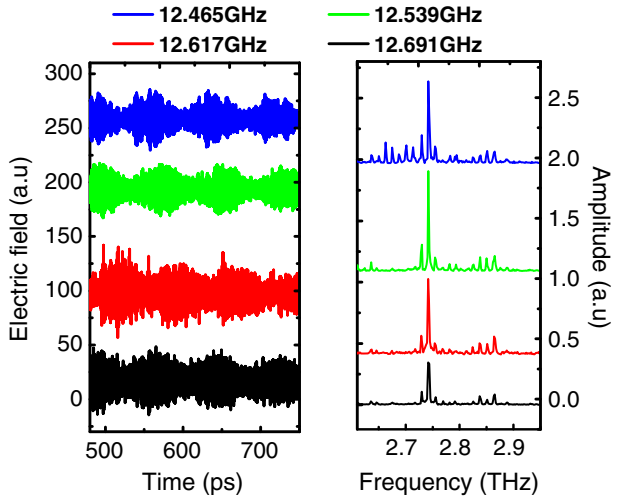

Fig. 3. QCL output electric field and the corresponding spectrum for microwave modulation frequencies of 12.465, 12.539, 12.617, and 12.691 GHz.

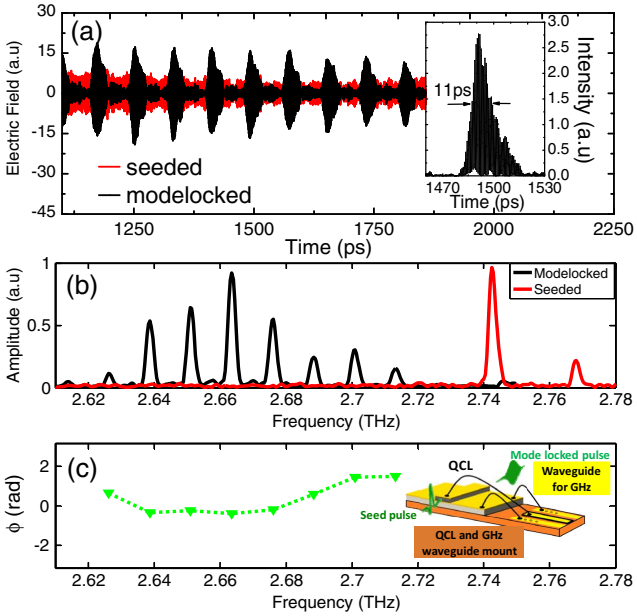

Fig. 4. Active mode locking and phase analysis of the MM QCL at 77 K. (a) Output electric field for the seeded (red) and mode-locked (black) QCLs with an applied microwave modulation of 12.46 GHz for the latter. Inset: expanded view of the THz pulse intensity between 1470 and 1530 ps. (b) FFT of panel (a) for a seeded (red) and a mode-locked (black) QCL. (c) Phases of the eight mode-locked longitudinal modes (green triangles). Inset: QCL schematic showing the device integrated with a microwave waveguide for active mode locking and illustrating the input seed pulse and the seeded/mode-locked output.

available in our current setup and showed the clearest pulse behavior (see below). The modulation frequency was varied between 12.4 and 14 GHz, with 12.465 GHz giving the best-quality pulses. Figure 3 shows the output electric fields and the corresponding spectra for various modulation frequencies (RF power of ~500 mW), which show that the pulse behavior becomes clearer and more Fabry–Perot modes appear as the microwave frequency is reduced. No clear pulse behavior was observed for frequencies greater than 12.7 GHz.

Figure 4(a) shows the electric field between 1100 and 1800 ps emitted by the seeded QCL with (black curve) and without (red curve) microwave modulation. The QCL was operated at 77 K and the electrical pulse power was chosen such that it brought the QCL above the laser threshold. (Compared with Fig. 3, the electrical pulse power was reduced to 450 mW, which led to shorter pulses and the pulse behavior was lost for other modulation frequencies.) As in Fig. 2, the output of the QCL without microwave modulation shows a quasi-continuous profile, resulting in only two modes visible in the FFT [Fig. 4(b)]. (The QCL is close to the threshold limiting the number of modes generated.) The situation changes drastically upon applying the microwave modulation, with clear generation of a pulse train. (The variation in intensity between the pulses in the time domain is a result of the nonflat RF electrical pulses and the low output fields of MM QCLs resulting in a low signal, close to the noise level.) The FFT shows the corresponding effect on the spectrum; eight uniformly spaced modes are observed between 2.61 and 2.72 THz. The average pulse width (in intensity) is found to be 11 ps as shown in the inset of Fig. 4(a). The number of modes and the pulse widths are larger and shorter, respectively, than those demonstrated from our previous investigations on bound-to-continuum active regions, showing the effect of the broader gain bandwidth of LO depopulation active region designs. However, the entire ~500 GHz bandwidth is not fully used. This is a result of the microwave modulation, which limits the pulse width and the number of modes—pulse formation is only present close to the laser threshold owing to the direct sinusoidal modulation of the QCL gain above and below the laser threshold (i.e., turning the QCL on and off rapidly), which limits the number of modes that can be brought above the threshold. Applying this microwave modulation when the quasi-DC current or the RF power supplying the QCL is closer to or above the laser threshold results in a sinusoidal amplitude modulation of the detected field, owing to the finite microwave power, with the pulse behavior destroyed [12].

The application of a round-trip modulation of 12.47 GHz for the shortest pulse generation is different from the mode spacing found in the QCL seeding and the beat note frequency ($\Delta\nu \sim 13.2$ GHz). From the mode spacing, we find THz group refractive indices of 3.871 and 3.665 for the mode-locked and seeded regimes, respectively. It has been shown previously that the QCL round trip can be locked to an RF synthesizer over a locking range of several hundred megahertz with moderate microwave powers ("injection pulling"), but it is a surprise that the 12.47 GHz modulation frequency generates the clearest pulses. This effect has also been observed in the THz spectra of the microwave modulated QCLs in Ref. [18] where more modes are brought above the threshold when a microwave modulation different from the round-trip frequency is applied. In our previous work on single-plasmon waveguides, pulses were generated over a wide range of round-trip modulations (12.5–13.3 GHz). The difference here comes from the MM waveguide, which brings an extra dispersion in the refractive index of the microwave modulation and permits a THz–GHz phase matching [19], where the effective microwave index is equal to the THz group refractive index, i.e., n_G (THz) $= n_{\text{eff}}$ (GHz). Although this phase matching has been discussed in the context of modulation bandwidth, its demonstration and impact on short-pulse generation had not

been envisaged. The microwave index depends strongly on the ridge width and microwave frequency [19], with a refractive index of approximately 3.9 for a 60-μm-wide ridge at 12 GHz (see Supplement 1 for a simulation of microwave mode and refractive index dispersion). This indicates that the velocity of the THz pulse envelope is dictated by the microwave modulation wave and it is this direct modulation close to the threshold that permits pulse generation. This phenomenon is also supported by the fact that pulse generation is only observed when the microwave modulation is applied from the cavity end of the QCL, suggesting that the microwave propagates in-phase with the THz pulse. This also explains why it is easier to mode-lock THz QCLs in comparison with mid-infrared QCLs as, for the latter, the group refractive index is smaller (∼3.3) than that in the THz range and, thus, a microwave modulation has a different velocity than the mid-infrared group velocity.

An advantage of injection seeding with phase-resolved pulses is that it permits access to the phase and amplitude of the emitted pulse train, allowing a complete analysis of the mode-locked pulse emission. As can be seen in Fig. 4(a), the mode-locked pulses are deformed from an ideal Gaussian profile. Taking the FFT of the pulse train permits the phase of each mode to be determined as shown in Fig. 4(c); the four central intense modes at 2.639, 2.651, 2.664, and 2.676 THz have the same phase, whereas the phase increases monotonically for the modes (2.626, 2.689, 2.701, and 2.714 THz) that are farther from the central frequency. This deforms the pulse from the transform-limited case. An improved pulse shape could be obtained by engineering the gain to have a flatter profile such that the group velocity dispersion is minimized [15] and to have improvements to the microwave modulation, which could be distorted by the inductance from the wire bonding.

5. DISCUSSION AND CONCLUSION

Our results on the mode locking of THz QCLs in MM waveguides show that (i) clear pulse generation is only observed when the THz group index is equal to the effective modal index of the microwave modulation; (ii) pulse generation is only observed close to the threshold, resulting in low-output THz fields; and (iii) a considerable increase in the gain bandwidth does not translate into much shorter pulses. Taken together, these three points suggest that pulse generation from QCLs arises from a direct microwave modulation above and below the laser threshold, and that the pulse width is limited by the sinusoidal microwave modulation. However, the ultrafast gain recovery time measured here, which we show does not limit pulse generation, can be used as an advantage to generate more intense and shorter pulses if short intense electrical pulses can be used to switch on the QCL gain. For example, a Gaussian or Lorentzian profile could be used. Although difficult to generate electronically, optically generated electrical pulses using ultrafast lasers combined with ultrafast materials are feasible and these could then be used to switch the QCL on subpicosecond time scales. Further techniques that could circumvent the current limitations would be the application of greater microwave power for higher pulse energies and the application of hybrid mode locking techniques to shorten the pulses to sub-10 ps values [20].

To conclude, we have demonstrated the seeding of THz QCLs with an LO phonon depopulation active region design, fabricated in MM waveguides. The ultrafast seeding permits access to the gain recovery time, which is shown to be faster than that in bound-to-continuum active region designs and approaches that in mid-infrared QCLs. Furthermore, we have shown that 11 ps mode-locked pulses can be generated from these MM QCLs, with the pulse width determined by the microwave modulation and the phase matching between the microwave phase velocity and the envelope of the THz emission. The pulse generation is not limited by the inherent QCL bandwidth. This work implies that for QCL mode locking (THz and mid-infrared), the fast gain recovery time does not limit pulse formation, as postulated in the simulations in Refs. [17,20], when a strong active modulation is applied at the correct frequency. Importantly, considerations need to be made to engineer the waveguide and refractive index dispersion to achieve phase matching. As well as pulse generation, this work could have an impact on more stable comb generation [15,21] when referenced to a microwave modulation. Owing to the MM geometry, the output fields were low in amplitude, but this could be improved considerably by the integration of planar horn antennas [22] designed for the active mode locking of such structures. Further, the QCL operating temperature and electrical power dissipation are compatible with liquid nitrogen or Stirling coolers.

Funding. Agence Nationale de la Recherche (ANR) (ANR-12-NANO-0014); Conseil Général de l'Essonne; Engineering and Physical Sciences Research Council (EPSRC); European Commission (EC) (FET Open ULTRAQCL 665158); European Research Council (ERC) (GEM, TOSCA); Royal Society; Wolfson Foundation.

See Supplement 1 for supporting content.

REFERENCES

1. R. Köhler, A. Tredicucci, F. Beltram, H. E. Beere, E. H. Linfield, A. G. Davies, D. A. Ritchie, R. C. Iotti, and F. Rossi, "Terahertz semiconductor-heterostructure laser," Nature **417**, 156–159 (2002).
2. L. Li, L. Chen, J. Zhu, J. Freeman, P. Dean, A. Valavanis, A. G. Davies, and E. H. Linfield, "Terahertz quantum cascade lasers with >1 W output powers," Electron. Lett. **50**, 309–311 (2014).
3. S. Fathololoumi, E. Dupont, C. W. I. Chan, Z. R. Wasilewski, S. R. Laframboise, D. Ban, A. Mátyás, C. Jirauschek, Q. Hu, and H. C. Liu, "Terahertz quantum cascade lasers operating up to 200 K with optimized oscillator strength and improved injection tunneling," Opt. Express **20**, 3866–3876 (2012).
4. C. Y. Wang, L. Kyznetsova, V. M. Gkortsas, L. Diehl, F. X. Kartner, M. A. Belkin, A. Belyanin, X. Li, D. Ham, and H. Schneider, "Mode-locked pulses from mid-infrared quantum cascade lasers," Opt. Express **17**, 12929–12943 (2009).
5. S. Barbieri, M. Ravaro, P. Gellie, G. Santarelli, C. Manquest, C. Sirtori, S. P. Khanna, E. H. Linfield, and A. G. Davies, "Coherent sampling of active mode-locked terahertz quantum cascade lasers and frequency synthesis," Nat. Photonics **5**, 306–313 (2011).
6. J. R. Freeman, J. Maysonnave, H. E. Beere, D. A. Ritchie, J. Tignon, and S. S. Dhillon, "Electric field sampling of modelocked pulses from a quantum cascade laser," Opt. Express **21**, 16162–16169 (2013).
7. J. E. Bowers, P. Morton, A. Mar, and S. W. Corzine, "Actively mode-locked semiconductor lasers," IEEE J. Quantum Electron. **25**, 1426–1439 (1989).
8. E. L. Portnoi, J. H. Marsh, and E. A. Avrutin, "Monolithic and multi-gigahertz mode-locked semiconductor lasers: constructions, experiments, models and applications," IEE Proc. **147**, 251–278 (2000).
9. L. A. Jiang, M. E. Grein, H. Haus, and E. P. Ippen, "Noise of mode-locked semiconductor lasers," IEEE J. Sel. Top. Quantum Electron. **7**, 159–167 (2001).

10. D. Oustinov, N. Jukam, R. Rungsawang, J. Madéo, S. Barbieri, P. Filloux, C. Sirtori, X. Marcadet, J. Tignon, and S. Dhillon, "Phase seeding of a terahertz quantum cascade laser," Nat. Commun. **1**, 1–6 (2010).
11. W. Maineult, P. Gellie, A. Andronico, P. Filloux, G. Leo, C. Sirtori, S. Barbieri, E. Peytavit, T. Akalin, J.-F. Lampin, H. E. Beere, and D. A. Ritchie, "Metal–metal terahertz quantum cascade laser with micro-transverse-electromagnetic-horn antenna," Appl. Phys. Lett. **93**, 183508 (2008).
12. J. R. Freeman, J. Maysonnave, N. Jukam, P. Cavalié, K. Maussang, H. E. Beere, D. A. Ritchie, J. Mangeney, S. S. Dhillon, and J. Tignon, "Direct intensity sampling of a modelocked terahertz quantum cascade laser," Appl. Phys. Lett. **101**, 181115 (2012).
13. J. Maysonnave, N. Jukam, M. S. M. Ibrahim, R. Rungsawang, K. Maussang, J. Madéo, P. Cavalié, P. Dean, S. P. Khanna, D. P. Steenson, E. H. Linfield, A. G. Davies, S. S. Dhillon, and J. Tignon, "Measuring the sampling coherence of a terahertz quantum cascade laser," Opt. Express **20**, 16662–16670 (2012).
14. J. R. Freeman, J. Maysonnave, S. Khanna, E. H. Linfield, A. G. Davies, S. S. Dhillon, and J. Tignon, "Laser-seeding dynamics with few-cycle pulses: Maxwell–Bloch finite-difference time-domain simulations of terahertz quantum cascade lasers," Phys. Rev. A **87**, 063817 (2013).
15. M. Rösch, G. Scalari, M. Beck, and J. Faist, "Octave-spanning semiconductor laser," Nat. Photonics **9**, 42–47 (2015).
16. W. Kuehn, W. Parz, P. Gaal, K. Reimann, M. Woerner, T. Elsaesser, T. Müller, J. Darmo, K. Unterrainer, M. Austerer, G. Strasser, L. R. Wilson, J. W. Cockburn, A. B. Krysa, and J. S. Roberts, "Ultrafast phase-resolved pump–probe measurements on a quantum cascade laser," Appl. Phys. Lett. **93**, 151106 (2008).
17. Y. Wang and A. Belyanin, "Active mode-locking of mid-infrared quantum cascade lasers with short gain recovery time," Opt. Express **23**, 4173–4185 (2015).
18. S. Barbieri, W. Maineult, S. S. Dhillon, C. Sirtori, J. Alton, N. Breuil, H. E. Beere, and D. A. Ritchie, "13 GHz direct modulation of terahertz quantum cascade lasers," Appl. Phys. Lett. **91**, 143510 (2007).
19. W. Maineult, L. Ding, P. Gellie, P. Filloux, C. Sirtori, S. Barbieri, T. Akalin, J.-F. Lampin, I. Sagnes, H. E. Beere, and D. A. Ritchie, "Microwave modulation of terahertz quantum cascade lasers: a transmission-line approach," Appl. Phys. Lett. **96**, 021108 (2010).
20. A. K. Wójcik, P. Malara, R. Blanchard, T. S. Mansuripur, F. Capasso, and A. Belyanin, "Generation of picosecond pulses and frequency combs in actively mode locked external ring cavity quantum cascade lasers," Appl. Phys. Lett. **103**, 231102 (2013).
21. A. Hugi, G. Villares, S. Blaser, H. C. Liu, and J. Faist, "Mid-infrared frequency comb based on a quantum cascade laser," Nature **492**, 229–233 (2012).
22. A. Brewer, J. R. Freeman, P. Cavalié, J. Maysonnave, J. Tignon, S. S. Dhillon, H. E. Beere, and D. A. Ritchie, "Coherent detection of metal–metal terahertz quantum cascade lasers with improved emission characteristics," Appl. Phys. Lett. **104**, 081107 (2014).